INTEGRATED OPTICAL CIRCUITS

Ivars Melngailis, et al

Massachusetts Instiute of Technology

Prepared for:

Electronic Systems Division

31 July 1973

UNCLASSIFIED
Security Classification

AD-769858

DOCUMENT CONTROL DATA - R&D

(Security classification of title, body of abstract and indexing annotation must be entered when the overall report is classified)

1. ORIGINATING ACTIVITY *(Corporate author)*
Lincoln Laboratory, M.I.T.

2a. REPORT SECURITY CLASSIFICATION
Unclassifled

2b. GROUP

3. REPORT TITLE
Integrated Optical Circuits

4. DESCRIPTIVE NOTES *(Type of report and inclusive dates)*
Semiannual Technical Summary Report - 1 January through 31 July 1973

5. AUTHOR(S) *(Last name, first name, initial)*
Melngailis, Ivars Spears, David L. Stillman, Gregory E. Wolfe, Charles M.

6. REPORT DATE
31 July 1973

7a. TOTAL NO. OF PAGES
-18

7b. NO. OF REFS
14

8a. CONTRACT OR GRANT NO. F19628-73-C-0002

b. PROJECT NO. ARPA Order 2074

c.

d.

9a. ORIGINATOR'S REPORT NUMBER(S)
Semiannual Technical Summary, 31 July 1973

9b. OTHER REPORT NO(S) *(Any other numbers that may be assigned this report)*
ESD-TR-73-251

10. AVAILABILITY/LIMITATION NOTICES
Approved for public release; distribution unlimited.

11. SUPPLEMENTARY NOTES
None

12. SPONSORING MILITARY ACTIVITY
Advanced Research Projects Agency, Department of Defense

13. ABSTRACT

A program has been initiated to develop materials and device technology in the two compound semiconductor systems $In_xGa_{1-x}As$-GaAs and $Hg_xCd_{1-x}Te$-CdTe which will form a base for integrated Optical Circuits (IOC) applications in the short wavelength (0.9 to 1.1 μm) infrared and the long wavelength (10.6 μm) regions, respectively.

In the $In_xGa_{1-x}As$-GaAs system, work has progressed toward integrating an $In_xGa_{1-x}As$ avalanche photodiode detector in a GaAs waveguide. An $AsCl_3$-H_2-Ga-In vapor-phase system which permits compositional grading has been used to obtain 20-percent InAs layers. Relatively low defect densities have been achieved by controlled growth of an intermediate graded alloy region between the GaAs substrate and the 20-percent alloy in order to avoid defect formation due to lattice mismatch. Uniform $In_xGa_{1-x}As$ Schottky barrier avalanche photodiodes with gains of 250, rise times of about 170 psec, and quantum efficiencies of 50 percent at wavelengths up to 1.1 μm have been fabricated. Measurements have been made to determine the electron and hole ionization coefficients in GaAs avalanche photodiodes in order to obtain an estimate of the ultimate wide-bandwidth performance of GaAs and InGaAs devices. In addition, several waveguide fabrication schemes for $In_xGa_{1-x}As$ IOC's have been investigated.

In the $Hg_xCd_{1-x}Te$-CdTe area an effort has been started to develop $Hg_xCd_{1-x}Te$ epitaxial growth techniques and waveguide, coupler, and acoustic frequency-shifter technology in CdTe. A vapor-phase epitaxial system has been designed, constructed, and encouraging results have been obtained in preliminary experiments of epitaxial $Hg_xCd_{1-x}Te$ growth on CdTe substrates. Proton bombardment has been used on high carrier concentration (10^{18} cm^{-3}) CdTe to achieve carrier removal in a layer adjacent to the surface and waveguiding in this proton-bombarded region at 10.6 μm has been demonstrated.

In a related program, $Hg_xCd_{1-x}Te$ photodiodes have been developed for heterodyne detection at 10.6 μm with a frequency cutoff of near 800 MHz and quantum efficiencies greater than 40 percent. It is planned to eventually incorporate similar diodes in a $Hg_xCd_{1-x}Te$-CdTe IOC heterodyne receiver.

14. KEY WORDS

Integrated Optical Circuits
$In_xGa_{1-x}As$-GaAs
vapor-phase system
epitaxial growth
heterodyne detection
avalanche photodiodes
$Hg_xCd_{1-x}Te$-CdTe
Schottky barrier
proton bombardment

UNCLASSIFIED
Security Classification

MASSACHUSETTS INSTITUTE OF TECHNOLOGY

LINCOLN LABORATORY

INTEGRATED OPTICAL CIRCUITS

SEMIANNUAL TECHNICAL SUMMARY REPORT
TO THE
ADVANCED RESEARCH PROJECTS AGENCY

1 JANUARY – 31 JULY 1973

ISSUED 24 OCTOBER 1973

The work reported in this document was performed at Lincoln Laboratory, a center for research operated by Massachusetts Institute of Technology. This work was sponsored by the Advanced Research Projects Agency of the Department of Defense under Air Force Contract F19628-73-C-0002 (ARPA Order 2074) and is being monitored by Air Force Cambridge Research Laboratories.

ABSTRACT

A program has been initiated to develop materials and device technology in the two compound semiconductor systems $In_xGa_{1-x}As$-GaAs and $Hg_xCd_{1-x}Te$-CdTe which will form a base for Integrated Optical Circuits (IOC) applications in the short wavelength (0.9 to 1.1 μm) infrared and the long wavelength (10.6 μm) regions, respectively.

In the $In_xGa_{1-x}As$-GaAs system, work has progressed toward integrating an $In_xGa_{1-x}As$ avalanche photodiode detector in a GaAs waveguide. An $AsCl_3$-H_2-Ga-In vapor-phase system which permits compositional grading has been used to obtain 20-percent InAs layers. Relatively low defect densities have been achieved by controlled growth of an intermediate graded alloy region between the GaAs substrate and the 20-percent alloy in order to avoid defect formation due to lattice mismatch. Uniform $In_xGa_{1-x}As$ Schottky barrier avalanche photodiodes with gains of 250, rise times of about 170 psec, and quantum efficiencies of 50 percent at wavelengths up to 1.1 μm have been fabricated. Measurements have been made to determine the electron and hole ionization coefficients in GaAs avalanche photodiodes in order to obtain an estimate of the ultimate wide-bandwidth performance of GaAs and InGaAs devices. In addition, several waveguide fabrication schemes for $In_xGa_{1-x}As$ IOC's have been investigated.

In the $Hg_xCd_{1-x}Te$-CdTe area an effort has been started to develop $Hg_xCd_{1-x}Te$ epitaxial growth techniques and waveguide, coupler, and acoustic frequency-shifter technology in CdTe. A vapor-phase epitaxial system has been designed, constructed, and encouraging results have been obtained in preliminary experiments of epitaxial $Hg_xCd_{1-x}Te$ growth on CdTe substrates. Proton bombardment has been used on high carrier concentration (10^{18} cm^{-3}) CdTe to achieve carrier removal in a layer adjacent to the surface and waveguiding in this proton-bombarded region at 10.6 μm has been demonstrated.

In a related program, $Hg_xCd_{1-x}Te$ photodiodes have been developed for heterodyne detection at 10.6 μm with a frequency cutoff of near 800 MHz and quantum efficiencies greater than 40 percent. It is planned to eventually incorporate similar diodes in a $Hg_xCd_{1-x}Te$-CdTe IOC heterodyne receiver.

Accepted for the Air Force
Eugene C. Raabe, Lt. Col., USAF
Chief, ESD Lincoln Laboratory Project Office

CONTENTS

INTEGRATED OPTICAL CIRCUITS

I. $In_xGa_{1-x}As$-GaAs INTEGRATED OPTICAL CIRCUITS

A. MATERIALS PREPARATION

1. Epitaxial Growth

The $In_xGa_{1-x}As$ material is grown epitaxially on GaAs substrates using an $AsCl_3$-H_2-Ga-In vapor-phase system which permits grading the epitaxial layers from GaAs to the desired composition. The lattice mismatch between $In_xGa_{1-x}As$ alloys and GaAs makes it difficult to grow high-quality epitaxial layers for the fabrication of avalanche photodiodes. For an alloy composition of 20% InAs, the lattice constant is about 1.4 percent larger than that of GaAs. If all of this lattice mismatch were relieved plastically, it would create about 10^{13} dislocations per cm^2. However, by grading the epitaxial layer from GaAs out to the desired composition, the strain due to lattice mismatch should be largely elastic, and good quality epitaxial layers should be obtained.

The $AsCl_3$-H_2-Ga-In vapor-phase reactor used to grow the alloys is shown schematically in Fig. 1. The two $AsCl_3$-H_2 flows over the gallium and indium melts are separately controlled by feedback control systems. Growth is initiated with zero flow over the indium melt, and this flow is then increased in a programmed manner so that the epitaxial layer is graded from GaAs to the desired composition of $In_xGa_{1-x}As$. When the flow for this composition is reached, it is maintained constant until the epitaxial layer is as thick as desired.

The presaturated indium and gallium melts[1] are controlled at a temperature of 850°C with the center mixing zone at about the same temperature. Epitaxial growth is obtained on the GaAs seeds at a temperature of 700°C in a gradient of about 8°C/cm. Under these conditions the alloy composition of the epitaxial layer is essentially determined by the flow rates of H_2 + $AsCl_3$ over the indium and gallium melts. Figure 2 shows the variation of alloy composition as a function of the ratio of the flow rate over the indium melt to the flow rate over the gallium melt for a total flow of 250 ml/min, 850°C melt temperatures, and a 700°C growth temperature. The two dashed lines indicate the approximate scatter in the data caused by other variables which have yet to be controlled. As can be seen, the variation plotted in Fig. 2 is approximately linear. Thus, for constant growth rate and a constant flow rate over the gallium melt, a linear increase with time in flow rate over the indium melt should produce an approximately constant gradient in alloy composition.

Epitaxial layers of $In_xGa_{1-x}As$ with a composition of about 20% InAs have been grown on {111} Ga, {111} As, and {100} GaAs seeds. With the growth parameters indicated above, growth rates were typically 0.3, 0.07, and 0.12 μm/min for {111} Ga, {111} As, and {100} surfaces, respectively. 20% InAs layers free of gross defect structure were obtained with compositional gradients of about 0.5 to 1.0% InAs/μm. Layers were usually prepared so that about one-half of the total thickness was graded in alloy composition and one-half was constant in alloy composition.

2. Defect Characterization

As expected for $In_xGa_{1-x}As$ alloys grown epitaxially on GaAs, the quality of the grown layers is critically dependent upon the amount of lattice mismatch which can be maintained elastic during

the growth process. This is manifested in the curvature of the wafer (epitaxy plus substrate) after growth, which indicates that with careful grading almost all of the lattice mismatch can be maintained elastic. Preliminary studies of the defect structure in the constant composition region of the better wafers reveal dislocation densities on the order of 10^6 to 10^7 per cm^2 and stacking fault densities on the order of 10^4 per cm^2. These values indicate that about 99.9999 percent of the lattice mismatch is maintained elastic with the grading and growth process currently being used.

Although these defect densities might be expected to be too high to achieve an appreciable yield of microplasma-free avalanche photodiodes, several factors tend to compensate for this: first, there is no indication that microplasmas are associated with stacking faults; second, the dislocations are not distributed randomly; and finally, there is not a one-to-one correlation between dislocations and microplasmas. Generally, these factors enable us to obtain an appreciable yield of good devices. However, it is clear that the major problems we have encountered so far in this alloy system are caused by lattice mismatch, and we are continuing to explore means of minimizing these defect densities.

B. DEVICE FABRICATION

1. $In_xGa_{1-x}As$ Avalanche Photodiodes

The present work on $In_xGa_{1-x}As$ avalanche photodiodes is an extension of a previous one-year program which was sponsored by the Air Force Avionics Laboratory for developing discrete 1.06-μm avalanche diodes for use in satellite communications. In the earlier program, $In_xGa_{1-x}As$ diodes with uniform gains of about 200 and response times less than 200 psec were fabricated; however, the response peak was limited to about 0.95 μm due to an insufficient indium concentration in the alloy. Following the improvements in epitaxial growth techniques, uniform Schottky barrier avalanche photodiodes with gains of 250, rise times of about 170 psec, and quantum efficiencies of 50 percent at wavelengths as long as 1.10 μm have been fabricated in $In_xGa_{1-x}As$ alloys during the past six months. The structure and fabrication method were the same as previously used for the GaAs devices.[2]

The spectral responsivities of two $In_xGa_{1-x}As$ avalanche photodiodes are shown in Fig. 3. Also shown in this figure are two dashed curves indicating the responsivity of a GaAs Schottky barrier diode and a Si p-n junction avalanche photodiode. Lines of constant quantum efficiency are shown for comparison with the spectral response curve. Although the GaAs and Si detectors have their peak response at about the same wavelength, the Si detector responds to much longer wavelengths since the long wavelength cutoff for Si is much more gradual than for the GaAs and $In_xGa_{1-x}As$ detectors because of the indirect bandgap in Si. The quantum efficiency of the Si detector at 1.06 μm is quite low, however. The alloy detector with $x = 0.17$ has a quantum efficiency at 1.06 μm that is more than twice that of Si, but it is clear that a slightly higher mole fraction of InAs is needed to obtain a peak responsivity at 1.06 μm. The detector with $x = 0.20$ has a peak response at about 1.11 μm. The structure in the two alloy detector curves is probably due to interference effects of the thin Pt Schottky barrier and a protective oxide coating. The measurements shown in this figure were made at low bias voltages where the multiplication was essentially unity, but for these $In_xGa_{1-x}As$ detectors which had a net bulk carrier concentration ($N_D - N_A$) of about 2×10^{16} cm^{-3} there is no significant change in the spectral response curve at high reverse bias voltages and high multiplication, in contrast to the GaAs detectors where an increase in reverse bias causes an increase in the response at longer wavelengths because of the Franz-Keldysh shift

of the absorption edge.[2] At the low frequencies used for these measurements (~1 kHz) the average gain of the $In_{0.17}Ga_{0.83}As$ device was approximately 300.

Since very large gains can be observed due to edge breakdown or microplasmas, the uniformity of the diode response under high gain was examined by scanning the active area with a focused HeNe (0.633-μm) laser and displaying the photoresponse on an oscilloscope. A photograph of the response profile of an $In_{0.17}Ga_{0.83}As$ diode, operating at a gain of about 100, obtained in this way is shown in Fig. 4. The general shape of the 5-mil-diameter device can be seen in the figure. The round area at the top where there is no response is due to the lead wire on this device which blocked a small part of the active area. At this gain, the photoresponse across the area of the diode is uniform to within about 20 percent. The small nonuniformities present are apparently due to inhomogeneities or defects in the crystal since they could not be identified with surface defects in the Schottky barrier. The photoresponse which appears at the perimeter of the device results from laser light which is scattered into the high-gain areas of the diode from the Au contact ring and is not actually edge response. Using this technique, we can routinely scan each photodiode, and reject those which show evidence of microplasmas, edge breakdown, or other defects.

The speed of response of the diodes was studied using a mode-locked Nd:YAG laser with a pulse repetition frequency of 275 MHz. The response of an $In_{0.17}Ga_{0.83}As$ avalanche photodiode operating at a gain of more than 250 with a 50-ohm sampling oscilloscope is shown in Fig. 5. At this speed of operation the gain was measured by attenuating the laser so that the signal could just be observed on the sampling oscilloscope at low reverse bias values and then taking the ratio of the signal at a given bias to that at low bias. Since the photocurrent tended to saturate at higher power levels, the measured gain corresponds to a lower limit obtainable with the device. The rise and fall times of the pulses are essentially equal, and a more detailed examination of the pulse indicates a 10- to 90-percent rise time (and fall time) of 175 psec, which corresponds to a bandwidth of 2 GHz. There was no detectable change in the rise and fall times with bias voltage (multiplication). This response time represents the total system response and is probably limited by the RC time constant of the 50-ohm load and the capacitance of this 5-mil-diameter device, although the actual rise and fall times of the laser have not been determined. The response time can probably be reduced somewhat while maintaining the same device area by optimizing the doping in the epitaxial layer so that the capacitance is made smaller while still avoiding transit time limitations.

2. Ionization Coefficient Measurements

A preliminary study of the noise performance of the $In_xGa_{1-x}As$ avalanche photodiodes indicates that the noise power varies much less rapidly than M^3, where M is the multiplication gain, and that the detector noise at a gain of 250 is lower than the noise of a state-of-the-art wideband amplifier with a 5-dB noise figure. An $M^{2.1}$ dependence of the noise power was previously observed in GaAs Schottky barrier photodiodes,[2] but other measurements on GaAs p-n junction avalanche photodiodes have yielded an M^3 variation.[3] The theory of McIntyre[4] predicts that the noise power will vary as M^3 if the hole and electron ionization coefficients are equal, and as M^2 if one is much greater than the other and the multiplication is initiated by the carrier with the higher coefficient. The ratio of the hole and electron ionization coefficients is also important relative to gain-bandwidth product limitations. Emmons[5] has shown that in p-i-n avalanche photodiodes, for $M \leq \beta/\alpha$, where β and α are the hole and electron ionization coefficients, respectively,

the bandwidth is limited by the transit time only, but that for $M \geq \beta/\alpha$ there is a corresponding decrease in the bandwidth for an increase in M. If we extend this treatment to the Schottky barrier diodes and use the measured rise time of 175 psec, we can estimate that $\beta/\alpha \gtrsim 50$. Since the measured rise time is limited by the RC time constant rather than the gain-bandwidth product, this is only a lower limit for β/α. It should be noted that this conclusion does not agree with several reports of equal ionization coefficients for electrons and holes in GaAs.[6,7]

Experiments are now under way to attempt to accurately measure α and β in GaAs and to determine their variation with electric field. The devices used for these measurements were fabricated so that the multiplications due to pure hole and pure electron injection could be measured in the same device.[8] Pt or Au Schottky barriers were formed on n-type GaAs by electroplating, and edge breakdown at the perimeter of the barrier was eliminated by a guard ring formed by proton bombardment. The devices were illuminated from the back by strongly absorbed 0.63-μm laser radiation to obtain pure hole injection or by 1.06- or 1.15-μm laser radiation to obtain pure electron injection by photoemission from the metal Schottky barrier. Preliminary results of these experiments indicate that the hole and electron ionization rates are not equal but that $\beta > \alpha$.

3. Waveguide Fabrication Schemes

Several different schemes for the fabrication of thin-film optical waveguides in the $In_xGa_{1-x}As$-GaAs materials system have been investigated. The two most feasible methods both rely on the small change in the index of refraction between two regions of material with different carrier concentrations. This discontinuity in carrier concentration can be created in two different ways: (1) by proton bombardment of heavily doped crystals which creates a high resistivity, low carrier concentration region, and (2) by the growth of high-purity epitaxial structures on heavily doped substrates. The second method seems most desirable because of the possibility of obtaining lower loss waveguides. Preliminary absorption measurements indicate that it may be possible to fabricate low-loss waveguides in GaAs for the transmission of room-temperature GaAs laser emission. This would be very desirable from the standpoint of the fabrication of more complicated integrated optical circuits.

During the next six-month period we will fabricate thin-film waveguides by the methods described above and incorporate an $In_xGa_{1-x}As$ photodiode in a waveguide for the detection of optical radiation in the waveguide. The performance will be evaluated at various wavelengths from 0.905 μm to 1.06 μm.

II. $Hg_xCd_{1-x}Te$-CdTe INTEGRATED OPTICAL CIRCUITS

A. MATERIALS PREPARATION

Problems associated with lattice mismatch are not expected to be as severe in the epitaxial growth of $Hg_xCd_{1-x}Te$ on CdTe as they are in the InGaAs-GaAs system. As an example, alloys with a composition of 80% HgTe have a lattice constant that is only 0.25 percent smaller than the lattice constant of CdTe. Nevertheless, it may still be necessary to utilize grading to achieve the best quality material.

Our initial attempt to develop an epitaxial $Hg_xCd_{1-x}Te$ capability utilized a vapor-phase flow system at atmospheric pressure, since a preliminary study suggested this as the most viable approach. A photograph of the quartz apparatus constructed for this purpose is shown in Fig. 6. The system is designed to transport the three constituent elements in a H_2 carrier gas and to suitably combine them in the vicinity of a CdTe seed. The two horizontal taper joint inputs placed side-by-side on the left end of the quartz apparatus are utilized to insert cadmium and tellurium boats. The three vertical taper joint inputs are H_2 inlets for each of the constituent element chambers. The other two vertical tubes without taper joints which connect to the larger chamber are the inlet and outlet for circulating oil which maintains the mercury in the inner chamber at a constant temperature. On the right end of the tube a near vertical seed holder is attached to a larger taper joint to facilitate insertion and removal of the seeds. In the center of the tube a mixing chamber is utilized to homogenize the mercury and cadmium vapors. The quartz tube is placed in a three-zone furnace to provide control over the cadmium, tellurium, and growth temperatures.

Although there are a number of problems to be resolved, initial results with this system have been encouraging in that some epitaxial growth of $Hg_xCd_{1-x}Te$ on CdTe has been achieved. With this technique there appears to be a sizable segregation of the mercury in the vapor phase. Also, alloy composition appears to be strongly dependent upon growth temperature. We are presently attempting to optimize the various system parameters (time, flow rates, temperatures, and temperature gradients) to reproducibly obtain epitaxial growth of alloys with the desired 80% HgTe composition.

B. DEVICE FABRICATION

Proton bombardment of CdTe was investigated to determine whether the free-carrier density can be reduced by this technique in order to form an optical waveguide for 10.6 μm. Preliminary results indicate that such waveguide structures can be formed by the use of 3-MeV high-energy protons.

In the proton bombardment technique which has previously been used to fabricate waveguides in GaAs for wavelengths in the vicinity of 1.15 μm, the dielectric constant in a region adjacent to the surface is increased by reducing the free-carrier concentration.[9,10] The waveguide thickness can be precisely controlled by varying the proton energy. For CdTe an increase in dielectric constant by almost 10 percent is estimated for a decrease in carrier concentration from $10^{18}/cm^3$ to $10^{17}/cm^3$. However, in order to achieve adequate waveguide thickness in CdTe for 10.6-μm wavelength, proton energies about ten times higher than the 0.3-MeV energy used for 1.15-μm guides in GaAs are required.

High-energy proton bombardment studies were carried out at 0.3, 1, 2, 2.5, and 3 MeV on indium-doped CdTe with 1.8×10^{18} carriers/cm^3 and on bromine-doped CdTe with 1.4×10^{18} carriers/cm^3. The proton-bombarded CdTe wafers were evaluated by capacitance measurements made with plated gold Schottky barriers. Bombardments of 10^{15} protons/cm^2 at 0.3 MeV through thin Schottky barriers revealed zero bias carrier depletion depths of about 2.4 μm, which was somewhat less than the 3.1-μm range of the protons. The measured depletion depth implied an average carrier density in the surface layer of about 2×10^{14}/cm^3 or a factor of about 10^4 reduction from the initial value of 1.4×10^{18}/cm^3. Differential capacitance-voltage data indicated concentrations from 5×10^{15}/cm^3 to 5×10^{16}/cm^3 at the bottom of the depletion region. Capacitance measurements on samples bombarded with 3-MeV protons at 10^{15}/cm^2 indicated a removal of 0.8×10^{18} carriers/cm^3 from the initial 1.8×10^{18}/cm^3 value. Similar bombardments in GaAs produced semi-insulating material, i.e., much higher dosages are required for CdTe.

A detailed study was carried out on a sample which had been subjected to three successive proton bombardments: 3 MeV (1×10^{15}/cm^2), 1 MeV (5×10^{15}/cm^2), and 2 MeV (5×10^{15}/cm^2). Figure 7(a) shows the differential proton energy loss expected from this bombardment sequence as a function of distance from the sample surface. The numerical values were taken from Janni's[11] tables (derived from the Bethe equations) for Sn, which has an atomic number between that of Cd and Te. Note the three, sharp, energy-dissipation peaks at 13, 37, and 69 μm corresponding to the range of the 1-, 2-, and 3-MeV protons, respectively. Capacitance measurements after the bombardment sequence revealed Schottky barrier depletion regions about 10 μm into the surface, which implied an average carrier concentration of 10^{13}/cm^3. By etching successive layers of material from the surface and replating gold Schottky barriers we were able to obtain the carrier concentration profile shown in Fig. 7(b). The data are presented in the form of boxes with the width corresponding to the uncertainty in distance and the height corresponding to the range of carrier concentrations obtained from measurements on the five to 10 15-mil-square Schottky barriers at each step.

Within the accuracy of the measurements there is a good correlation between the calculated proton energy loss profile and the measured carrier concentration profile. Pronounced minima in carrier concentration occur exactly at the expected ranges of the 2- and 3-MeV protons with the 2-MeV minima being much deeper, which is consistent with the 5 times higher dosage at 2 MeV than at 3 MeV. About 0.5×10^{24} eV/cm^3 of proton energy loss is required to remove 50 percent of 1.4×10^{18} carriers/cm^3, or about 0.3 MeV/carrier. However, upon comparison of the two plots of Fig. 7 it appears that this factor scales inversely as the residual carrier density, so at 10^{16}/cm^3, about 30 MeV/carrier, is required. Thus, much higher proton dosages than those for GaAs are needed to convert this material into semi-insulating CdTe, if indeed it can be done by proton bombardment. This may require starting with a CdTe crystal which is not saturation-doped with impurities as were the wafers used in our experiments. Fortunately, for an optical waveguide, it is not necessary to have a semi-insulating layer. Since the refractive index change is proportional to the change in carrier concentration, a residual level of 10^{16}/cm^3 should not seriously affect waveguiding. The free-carrier optical absorption coefficient at 10 μm in our starting material was measured to be about 400 cm^{-1}, but for a carrier concentration of 10^{15}/cm^3 it is less than 1 cm^{-1} (Ref. 12).

Attempts have been made to detect waveguiding in the proton-bombarded structures by cleaving the edges of the wafers and focusing a 10.3-μm CO_2 laser beam onto one edge with an f/10 germanium lens. Samples which had been bombarded with 2.5-MeV protons at a dose of 10^{16}/cm^2

showed as much as 10 percent transmission through a 1.6-mm path length and 1 percent transmission through a 3-mm path, although considerable variation in transmitted light was observed from one part of the sample to another. The two transmission measurements correspond to estimated waveguide losses of 6 and 11 cm^{-1}, respectively, when taking into account the focal spot size of the incident laser beam relative to the estimated 53-μm guide thickness and reflection losses, i.e., the effective absorption coefficient has been reduced by about two orders of magnitude from that of the bulk crystal. Figure 8 shows the transmission profile of the 1.6-mm sample. We are presently investigating ways of further reducing the attenuation and improving waveguide uniformity.

A grating coupler photomask pattern has been designed and constructed. The grating has $2\frac{1}{2}$-μm linewidths and spacings and should couple into the guides at an angle of incidence of about 33°. We are presently working on the parameters for sputter-etching these patterns into the CdTe samples.

Surface acoustic wave transducer patterns with 10.2-μm periodicity have been designed and fabricated onto semi-insulating CdTe substrates. Since the bulk shear wave velocity in CdTe is 1.85×10^3 m/sec (Ref. 13) we expect these devices to generate about 160-MHz surface waves in the material. The transducer pattern was designed to have a ZnO film overlay to improve the approximately 1-ohm radiation impedance which is calculated for the optimum CdTe transducer. From previous work on ZnO overlays on GaAs substrates,[14] we expect to obtain at least a factor of 10 increase in radiation impedance. Work is in progress to incorporate the ZnO overlay into the transducer structure.

$Hg_xCd_{1-x}Te$ 10.6-μm High-Speed Photodiodes

In a related program funded by the Air Force line item with additional support by DARPA-STO, $Hg_xCd_{1-x}Te$ photodiodes have been developed for heterodyne detection at 10.6 μm. The diodes were fabricated by Hg-diffusion into p-type crystals with an alloy composition of about 19% CdTe. Diodes in the form of etched mesas 250 μm in diameter were packaged and tested. External quantum efficiencies for diodes operated at 77°K were typically 40 to 50 percent (uncoated) over the 9- to 11-μm region, with zero bias low-frequency detectivities as high as 1.1×10^{10} $cmHz^{1/2}/W$. Frequency response measurements were made by heterodyning a tunable PbSnTe diode laser with a fixed-frequency CO_2 laser. The 3-dB rolloff point into a 50-ohm preamplifier was over 800 MHz with 0.8 V reverse bias. Local oscillator-noise-limited operation was observed at 400 MHz with about one milliwatt of CO_2 laser power. It is planned to eventually incorporate similar diodes in a $Hg_xCd_{1-x}Te$-CdTe IOC for heterodyne detection at 10.6 μm.

REFERENCES

1. R. N. Hall, J. Electrochem. Soc. 110, 385 (1963).
2. W. T. Lindley, R. J. Phelan, Jr., C. M. Wolfe and A. G. Foyt, Appl. Phys. Letters 14, 197 (1969).
3. T. Igo and Y. Toyoshima, Japan J. Appl. Phys. 9, 1286 (1970).
4. R. J. McIntyre, IEEE Transactions on Electron Devices ED-13, 164 (1966).
5. R. B. Emmons, J. Appl. Phys. 38, 3705 (1967).
6. R. A. Logan, A. G. Chynoweth and B. G. Cohen, Phys. Rev. 128, 2518 (1962).
7. R. A. Logan and S. M. Sze, Proc. Int. Conf. Phys. of Semiconductors, Kyoto, J. Phys. Soc. Japan 21, Supplement, 434 (1966).
8. M. H. Woods, W. C. Johnson and M. A. Lampert, Solid State Electron. 16, 381 (1973).
9. A. G. Foyt, W. T. Lindley, C. M. Wolfe and J. P. Donnelly, Solid State Electron. 12, 209 (1969).
10. E. Garmire, H. Stoll, A. Yariv and R. G. Hunsperger, Appl. Phys. Letters 21, 87 (1972).
11. J. F. Janni, Air Force Weapons Laboratory Technical Report No. AFWL-TR-65-150 (September 1966).
12. Solid State Research, Lincoln Laboratory, M.I.T. (1972:2), p. 23, DDC AD-748836.
13. H. J. McSkimin and D. G. Thomas, J. Appl. Phys. 33, 56 (1962).
14. Solid State Research, Lincoln Laboratory, M.I.T. (1971:4), p. 13, DDC AD-736501.

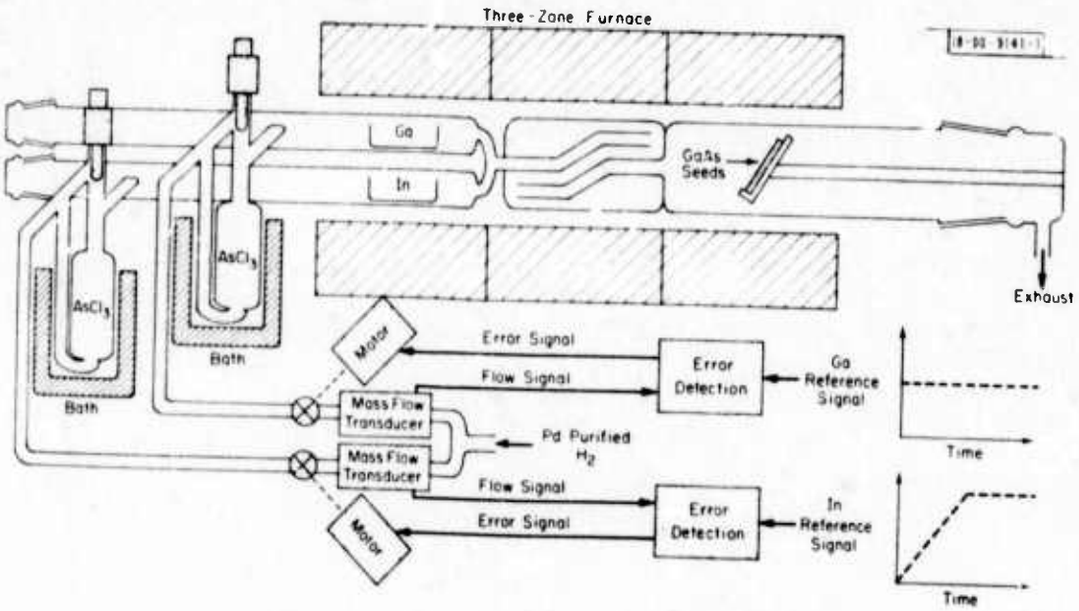

Fig. 1. Schematic diagram of the epitaxial $In_xGa_{1-x}As$ growth system.

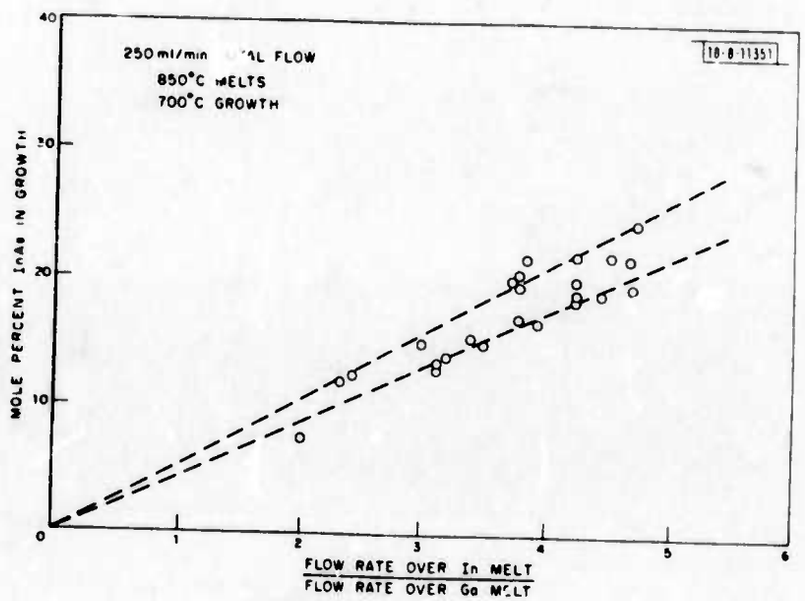

Fig. 2. Mole percent InAs in the epitaxial layer as a function of the ratio of the flow rate of $H_2 + AsCl_3$ over the indium melt to the flow rate over the gallium melt.

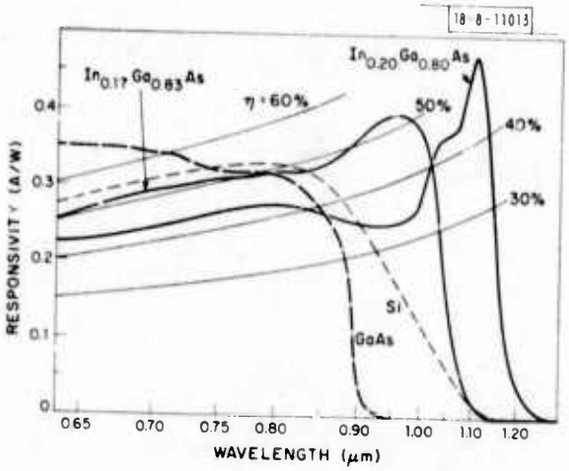

Fig. 3. Spectral responsivity of two $In_xGa_{1-x}As$ avalanche photodiodes at unity gain.

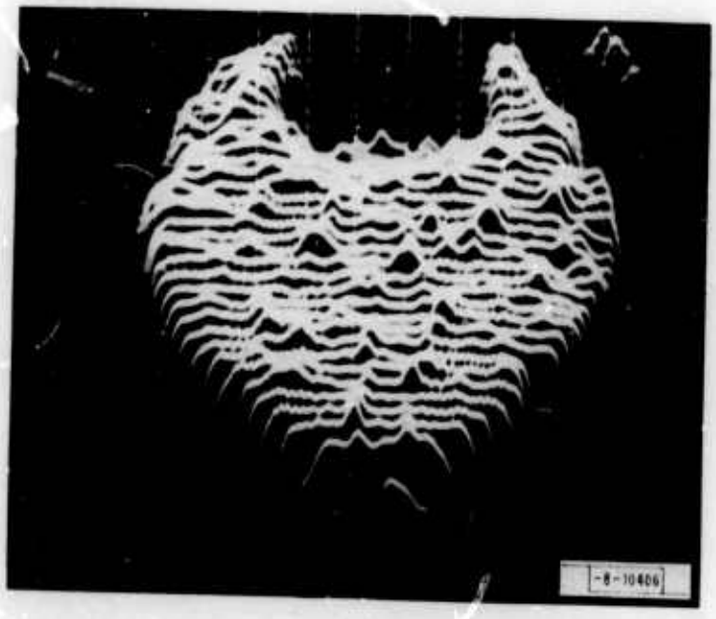

Fig. 4. Response profile of an $In_{0.17}Ga_{0.83}As$ avalanche photodiode operating at a gain of 100 when scanned with a HeNe 0.633-μm laser.

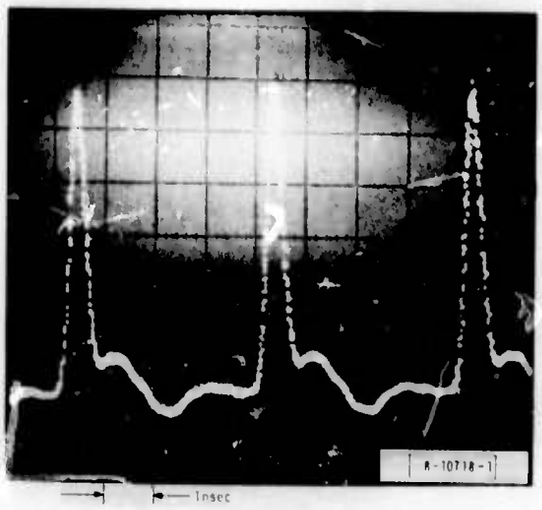

Fig. 5. Transient response of an $In_{0.17}Ga_{0.83}As$ avalanche photodiode excited by a 1.06-μm mode-locked Nd:YAG laser. This photograph was obtained from a 50-ohm sampling oscilloscope, and the device was operating at a gain greater than 250.

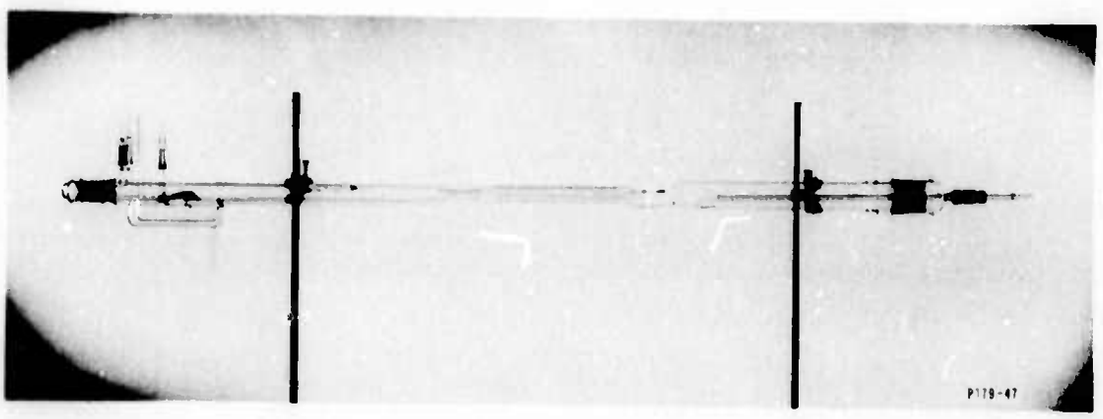

Fig. 6. Photograph of quartz apparatus for the growth of epitaxial $Hg_xCd_{1-x}Te$.

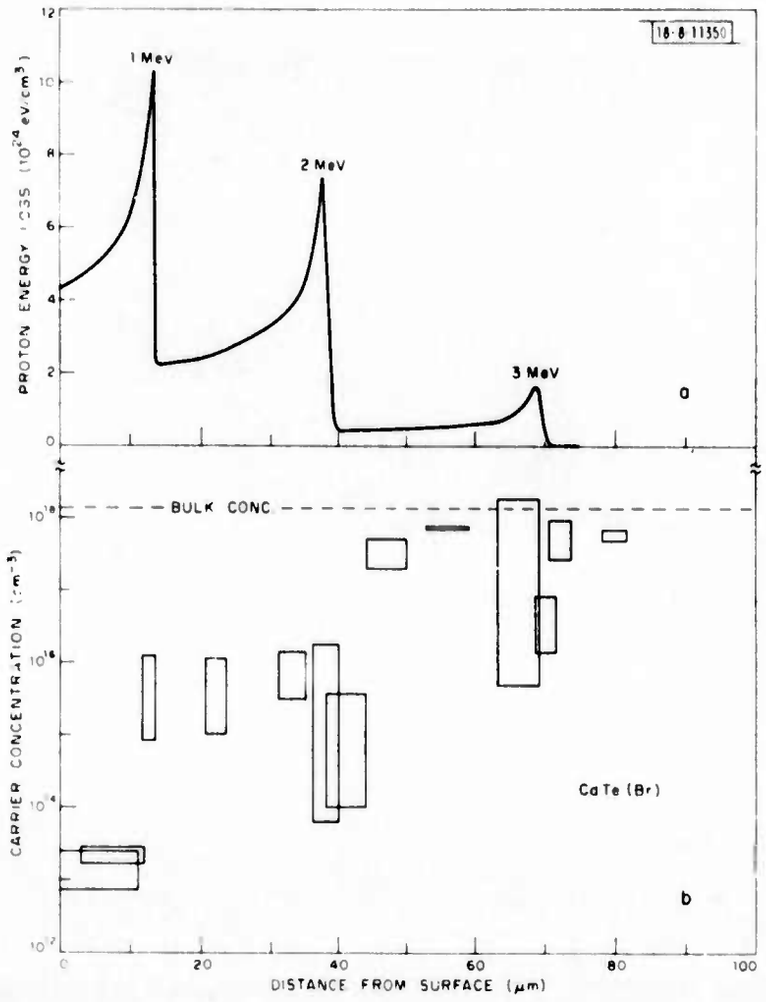

Fig. 7. (a) Theoretical proton energy loss as a function of distance from the surface for a CdTe sample subjected to three successive bombardments:

1 MeV (5×10^{15}/em^2);

2 MeV (5×10^{15}/cm^2);

3 MeV (1×10^{15}/em^2).

(b) The carrier concentration profile determined by Schottky barrier capacitance measurements after the above bombardment sequence.

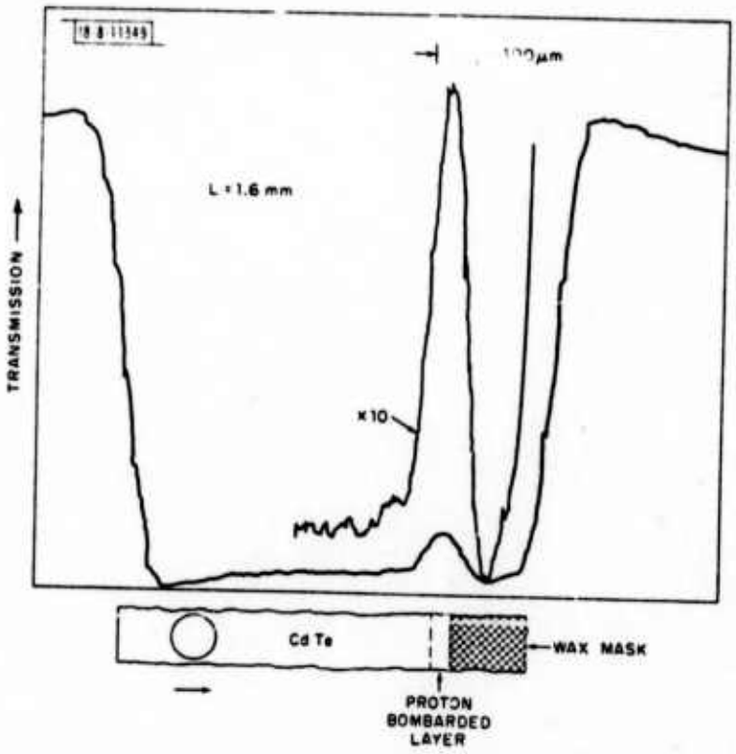

Fig. 8. Transmission profile of CO_2 laser radiation across a 1.6-mm-long CdTe sample with a 53-μm-deep waveguide region produced by 2.5-MeV proton bombardment.